Letter | Editors' Suggestion

Signatures of a quantum critical endpoint in the Kitaev candidate $Na_2Co_2TeO_6$

J. Arneth [1,*] K.-Y. Choi [2] R. Kalaivanan,[3] R. Sankar [3] and R. Klingeler [1,†]

[1]*Kirchhoff Institute for Physics, Heidelberg University, INF 227, D-69120 Heidelberg, Germany*

[2]*Department of Physics, Sungkyunkwan University, Suwon 16419, Republic of Korea*

[3]*Institute of Physics, Academia Sinica, Taipei 11529, Taiwan*

(Received 26 April 2024; revised 24 July 2024; accepted 11 September 2024; published 2 October 2024)

The putative Kitaev material $Na_2Co_2TeO_6$ has recently been proposed to enter a quantum spin disordered state when magnetic fields are applied in parallel to the honeycomb layers. In this Letter we uncover signatures of a quantum critical endpoint (QCEP) associated with the assumed order-disorder transition by means of high-resolution capacitance dilatometry. At the critical field $B_C \simeq 6$ T, a sign change of the out-of-plane thermal expansion coefficient α_c indicates the accumulation of entropy upon crossing the phase boundary. The proportional relationship between isothermal magnetization and magnetostriction signals that the QCEP can be tuned by magnetic field and pressure simultaneously. The presented results expand the material classes that exhibit metamagnetic quantum criticality to honeycomb antiferromagnets with possible Kitaev interactions.

DOI: 10.1103/PhysRevB.110.L140402

Within the framework of the everlasting search for a quantum spin liquid (QSL), the exactly solvable Kitaev model offers a promising route to a long-range entangled yet magnetically disordered state with exotic elementary excitations, such as Majorana fermions [1]. At the heart of this model lie strongly anisotropic, bond-dependent Ising interactions in a $S = 1/2$ honeycomb network, leading to pronounced magnetic frustration. The first wave of Kitaev candidate materials consisted of d^5 transition metal ions with strong spin-orbit coupling (SOC) situated in edge-sharing anion octahedra [2,3]. Among many experimental results arising from such theoretical proposals especially the $5d$ iridate Na_2IrO_3 and the $4d$ ruthenate α-$RuCl_3$ have managed to stand out, since both exhibit promising characteristics hinting at proximity to the QSL phase [4–6].

However, over time the list of materials possibly realizing the Kitaev model has also expanded to include cobaltates with a high-spin d^7 electronic configuration [7–9]. In these systems the presence of spin-active e_g electrons is suggested to reduce the strength of Heisenberg interactions J, thereby enhancing the dominance of the Kitaev contributions. Out of these "second wave" materials, $Na_2Co_2TeO_6$ has quickly been regarded as the most promising compound due to its notable similarities to α-$RuCl_3$: Even though $Na_2Co_2TeO_6$ exhibits magnetic long-range order below $T_N = 27$ K, the first reported antiferromagnetic zigzag ground state [10]—recently revised as a triple-**q** order [11,12]—is a promising indication of a proximate QSL state, as these two phases are adjacent in the parameter space of the Kitaev-Heisenberg model [13]. Indeed, a discontinuous phase transition appears when a magnetic field of $B_C \sim 6$ T is applied along the direction of the nearest-neighbor Co-Co bonds [14,15]. Despite the lack of knowledge about the exact magnetic ground state in the high-field phase of $Na_2Co_2TeO_6$, the experimental and theoretical results suggest the emergence of magnetic disorder at the critical field [16–18].

Here, we further highlight the intriguing effects of in-plane magnetic fields on $Na_2Co_2TeO_6$ by showing that the first-order phase transition at B_C exhibits strong signatures of quantum critical behavior close to a quantum critical endpoint (QCEP). The role of magnetoelastic coupling is elucidated by thermal expansion and magnetostriction measurements between 2 and 300 K and up to 15 T on high-quality single crystals of $Na_2Co_2TeO_6$ grown as described in Ref. [19]. Note that the presence of a potential antiferromagnetic impurity phase [20] is ruled out by our magnetization data (cf. Supplemental Material [21]). Out-of-plane relative length changes dL_c/L_c, i.e., along the crystallographic c direction, were studied on a 0.145-mm-thin single crystal by means of a three-terminal high-resolution capacitance dilatometer (Kuechler Innovative Measurement Technology) in a home-built setup placed inside a variable temperature insert of an Oxford magnet system [22,23]. From the relative length changes the linear thermal expansion coefficient $\alpha_c = 1/L_c \times (\partial L_c/\partial T)$ was derived. Magnetic fields were applied along the direction of first-neighbor Co-Co bonds ($B||a^*$) within the hexagonal planes. Thermal expansion and magnetostriction measurements were performed at rates of 0.3 K/min and 0.3 T/min, respectively. The magnetization was studied by means of a physical properties measurement system (PPMS, Quantum Design) using the vibrating sample magnetometer (VSM) option.

The low-temperature out-of-plane thermal expansion of $Na_2Co_2TeO_6$ is shown in Fig. 1 for representative magnetic fields $B||a^*$.[1] In zero magnetic field, the c axis continuously shrinks upon cooling, but notably, it also shows a sharp kink at

*Contact author: jan.arneth@kip.uni-heidelberg.de

†Contact author: klingeler@kip.uni-heidelberg.de

[1]The measurements have been performed following a field-cooled (FC) protocol where the sample was cooled in the applied field.

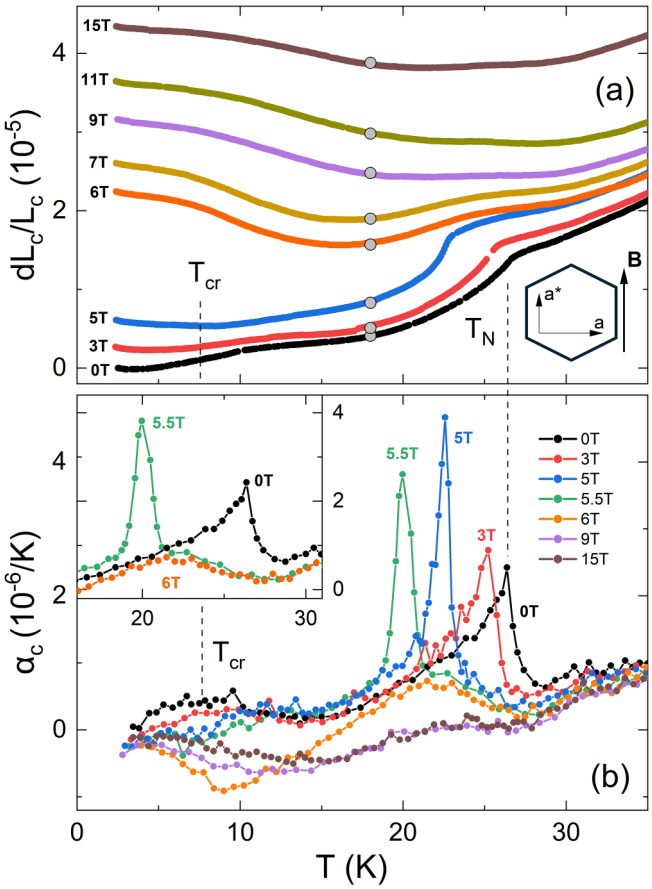

FIG. 1. (a) Out-of-plane thermal expansion dL_c/L_c and (b) linear thermal expansion coefficient α_c for both zero and finite magnetic fields applied $B||a^*$. As a reference point, $L(T = 2\ \mathrm{K}; B = 0\ \mathrm{T})$ is set to zero and data at different fields in (a) are scaled according to the magnetostriction measurements at 18 K (gray markers; see Fig. 3). T_N and T_{cr} mark the evolution of long-range magnetic order and the additional hump in zero field. Inset: Anomalies in α_c at T_N for $B = 0$, 5.5, and 6 T.

the antiferromagnetic ordering temperature $T_N = 26.8(3)$ K, which is reflected by a corresponding λ-shaped peak in the thermal expansion coefficient α_c [Fig. 1(b)]. The pronounced anomaly unambiguously indicates significant coupling between spin and lattice degrees of freedom in $Na_2Co_2TeO_6$. Interestingly, at around $T_{cr} = 7.5(9)$ K, another steplike feature can be found in the thermal expansion data as well as a corresponding broad hump in α_c. Note that the observation of a λ-shaped anomaly at T_N and a broad hump at T_{cr} resembles the overall behavior of the specific heat capacity c_p of $Na_2Co_2TeO_6$ as reported in Ref. [15]. In their study Yao *et al.* attribute the broad hump at T_{cr} to magnetic interplane correlations that remain short ranged due to Na disorder in separating layers.

While the thermal expansion coefficient at temperatures above T_N is not particularly sensitive to magnetic fields applied along the a^* axis, the anomaly at T_N shifts to lower temperatures and becomes more pronounced in magnetic fields up to 5 T. Concomitantly, the initially λ-shaped anomaly evolves into an even more pronounced symmetric peak and a small preceding steplike feature [see $\alpha_c(5.5\ \mathrm{T})$ in the inset in Fig. 1(b)]. The observed symmetric peak-shaped anomaly implies an associated jump in L_c, i.e., a first-order phase transition. At fields $B \geqslant 6$ T, a clear anomaly is no longer visible in the length changes and in α_c only the small steplike increase can be identified. Also for the humplike feature at T_{cr}, two field regimes can be identified: For $B \leqslant 5$ T, the steplike shrinking of the c axis continuously diminishes with increasing external magnetic field while it reappears for $B \geqslant 6$ T, albeit now signaling an anomalous *increase* in length [Fig. 1(a)]. Eventually, at $B > 10$ T, the c axis only weakly depends on temperature $T < 30$ K and α_c is independent on the applied field in this regime (see the Supplemental Material [21] for all thermal expansion data). For the further analysis of the data, we hence use $\alpha_c(15\ \mathrm{T})$ as an estimate of the nonmagnetic thermal expansion, since at such high fields the spins are completely polarized at sufficiently low temperatures. Similar methods have been used in the literature, e.g., in the closely related honeycomb magnet α-$RuCl_3$ [24].

We particularly emphasize the field dependence of the thermal expansion around T_{cr}: It is already evident from the c-axis dependence in Fig. 1(a) that α_c shows a sign change from positive at small fields to negative at fields $B \geqslant 6$ T. At intermediate fields around 5.5 T the thermal expansion coefficient almost vanishes below 10 K. The field effects are particularly visible when considering the thermal expansion coefficient as a function of B at fixed temperature of $T = 8$ K as shown in Fig. 2(a) (for other temperatures see the Supplemental Material [21]).[2] Here, we also plot the bare magnetic contribution $\alpha_c^{\mathrm{mag}} = \alpha_c - \alpha_c^{\mathrm{nonmag}}$ by using $\alpha_c^{\mathrm{nonmag}} \simeq \alpha_c(15\ \mathrm{T})$. Both data sets clearly imply a sign change in thermal expansion at $B_C(8\ \mathrm{K}) \simeq 5.5$ T which coincides well with the field-driven first-order phase transition occurring in the same field range [15,16,25,26].

In recent literature, the corresponding discontinuity in the magnetization at B_C has been attributed to an order-disorder transition into a QSL-like state [16]. Here, we uncover another intriguing property of the anomalous behavior at B_C, that is, its distinct signatures of quantum criticality. Since the linear thermal expansion coefficient is directly proportional to the pressure dependence of the entropy via the Maxwell relation $\alpha_c \sim \partial S/\partial p_c|_T$, a sign change of α_c upon the application of magnetic fields implies a maximum of the magnetic contribution to the entropy at B_C. Such an accumulation of S_{mag} is regularly expected to occur at a quantum critical point (QCP) [27–29]. It is important to note that the here reported quantum criticality, and hence also its critical properties, differs from the commonly discussed ones in the way that the underlying phase transition is not continuous but of a first-order type. In this scenario the so-called metamagnetic quantum critical endpoint (QCEP) is understood to be the endpoint of a line of a first-order phase transition when the temperature is reduced to zero [27,28,30]. Our interpretation is further supported by the data in Ref. [31], the detailed

[2]At $T = 8$ K, zero-field thermal expansion shows a hump associated to pronounced critical fluctuations so that the effects of magnetic fields can be expected to be particularly large. In addition, at lowest temperatures, thermal expansion vanishes so that the signal-to-noise ratio decreases at lowest temperatures under study.

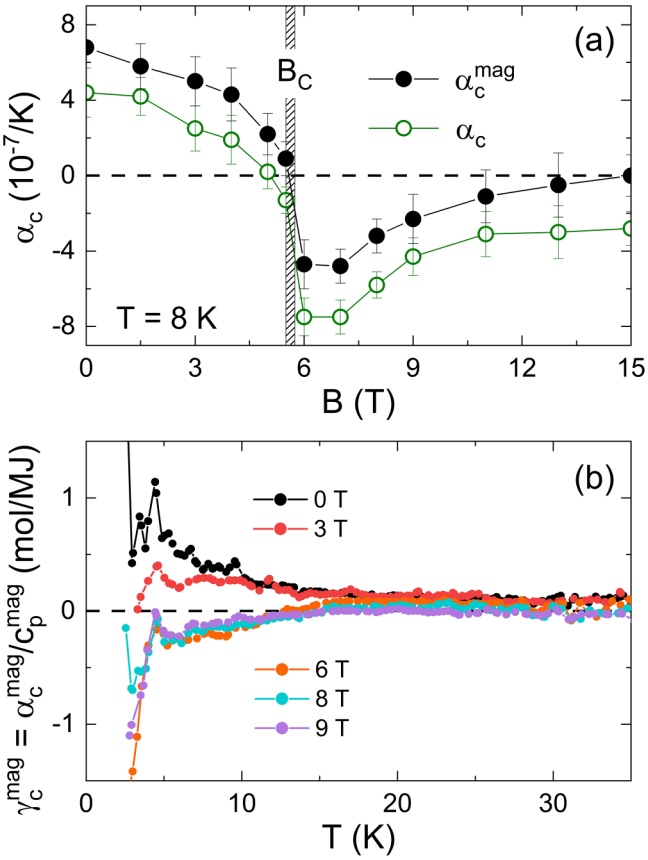

FIG. 2. (a) Out-of-plane linear thermal expansion coefficient and its magnetic contribution at 8 K as a function of magnetic field. The vertical dashed region marks the first-order phase transition at B_C. (b) Temperature dependence of the unidirectional magnetic Grüneisen parameter γ_c^{mag}, obtained by dividing the magnetic contributions to α_c and c_p from Ref. [15], at selected magnetic fields applied along the a^* axis.

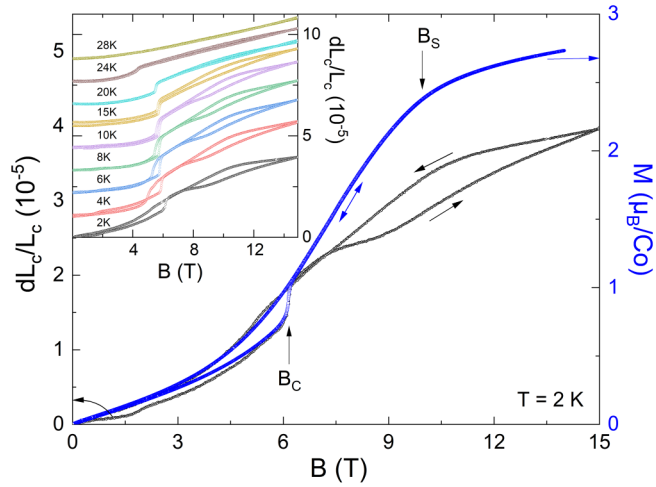

FIG. 3. Isothermal magnetostriction $L_c(B)$ (black) and magnetization $M(B)$ (blue) at $T = 2$ K for $B||a^*$. Arrows denote the direction of the field sweep. The inset depicts magnetostriction measurements at various temperatures, which are shifted along the ordinate. B_C and B_S mark the critical field and the saturation field, respectively.

inspection of which shows that the in-plane thermal expansion coefficient α_{a^*} changes its sign, too, at $B||a^* = 6$ T [31].

A key signature of metamagnetic quantum criticality is a sign change of the magnetic Grüneisen parameter, which is defined as the ratio of the magnetic contributions to the thermal expansion coefficient and the specific heat capacity $\gamma_{mag} = \alpha^{mag}/c_p^{mag}$ [27,28,32]. Figure 2(b) shows the uniaxial magnetic Grüneisen parameter of $Na_2Co_2TeO_6$ at representative magnetic fields as calculated from our thermal expansion data and the specific heat capacity measured in Ref. [15]. The resulting Grüneisen ratio is close to zero at $T > 20$ K but continuously increases upon cooling for $B \leqslant 5$ T. The opposite trend appears for $B \geqslant 6$ T. Extrapolating the temperature dependence for $T \to 0$ the data indicate a divergence at zero temperature, which can, however, not be seen directly in the data due to limited resolution and tiny length changes at low temperatures.

Signatures of metamagnetic quantum criticality as described in the present Letter have been first found and discussed in $Sr_3Ru_2O_7$ [32–34]. Later on, a sign change of the out-of-plane thermal expansion coefficient connected to a first-order phase transition was also observed in $CeRu_2Si_2$ [35,36] and in $Ca_{1.8}Sr_{0.2}RuO_4$ [37]. Additionally, indications of QCEPs were found in UGe_2 [38], UCoAl [39], and $ZrZn_2$ [40]. To our knowledge, metamagnetic quantum criticality has been reported exclusively in itinerant electron systems, which highlights the finding of $Na_2Co_2TeO_6$ exhibiting a quantum critical endpoint as an antiferromagnetic insulator. At this point it is noteworthy that thermal expansion in the closely related Kitaev candidate α-$RuCl_3$ also hints at the emergence of a quantum phase transition at B_C, which is debated to precede a QSL state [24]. In α-$RuCl_3$, however, the transition into the putative magnetically disordered phase exhibits a rather continuous character, which leads to differing quantum critical properties as compared to $Na_2Co_2TeO_6$.

The coupling of spin and lattice degrees of freedom can be also directly studied through magnetostriction experiments. Figure 3 shows the relative out-of-plane length changes (black) and the isothermal magnetization (blue) of $Na_2Co_2TeO_6$ at 1.8 K for $B||a^*$. As can be seen, the discontinuity in the magnetization is accompanied by a positive jump in the c-axis length, suggesting that both magnetic field and uniaxial pressure can be used as tuning parameters of the QCEP [27]. At $B_S(2\text{ K}) \simeq 10$ T, the magnetization implies the evolution of the polarized spin configuration. Similar to the field region around B_C, dL_c exhibits pronounced differences between the up- and down-sweep of the magnetic field starting from 8 T, while no corresponding hysteresis is observed in the magnetization data. As depicted in the inset of Fig. 3, the hysteresis region at $B_C(T)$ narrows as the temperature is increased and totally vanishes at $T \geqslant T_N$. Notably, hysteresis in magnetostriction above $B_C(T)$ ranges well beyond $B_S(T)$ and persists up to at least 24 K, i.e., in the whole reported quantum disordered regime [16]. The hysteresis diminishes but the hysteretic field range does not shrink upon heating. This indicates magnetostructural domain effects rather than a weak first-order character of the phase boundary $B_S(T)$. In addition, the magnetostriction exhibits a weak discontinuity of unknown origin at $B \simeq 1.5$ T when the field is increased from zero, but not when the field is subsequently decreased. At

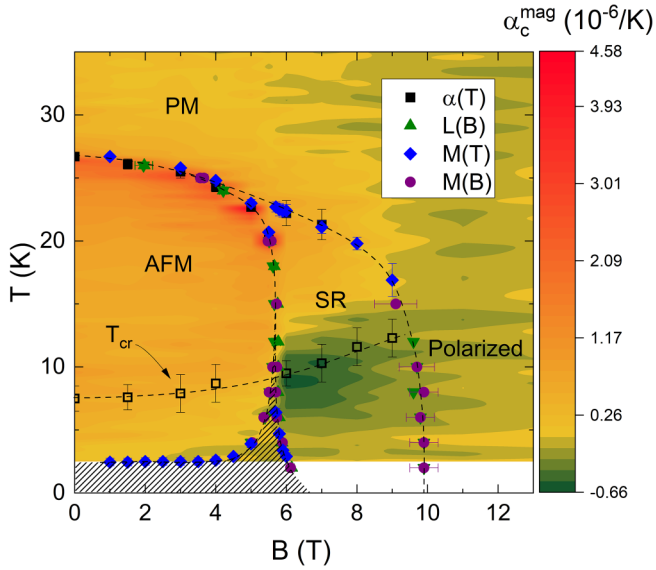

FIG. 4. Magnetic phase diagram of $Na_2Co_2TeO_6$ for magnetic fields applied $B||a^*$ as constructed from magnetic and dilatometric measurements. PM, AFM, and SR denote the paramagnetic, canted antiferromagnetic, and spin reoriented phase, respectively. The hatched area shows the hysteresis region observed in M and L_c (see the text). Additionally, $\alpha_c^{mag}(T, B)$ is depicted in color scale. The distinct data sets are shown in the Supplemental Material [21].

intermediate temperatures around 6 K this results in crossing of the up- and down-sweep magnetostriction at approximately 5.5 T.

Noteworthy, field-induced magnetization and length changes, at 2 K, closely track each other, i.e., the curves can be well overlapped by a single scaling factor, up to the critical field B_C. This observation parallels the findings of magnetostriction measurements on $Sr_3Ru_2O_7$ [34] and $CeRu_2Si_2$ [36]. Following the arguments discussed in that frame, such a good proportionality of $M(B)$ and $L_c(B)$ implies that variations in uniaxial pressure and magnetic field probe the same thermodynamic information as expected in a quantum critical regime [27]. Hence, the magnetostriction data strongly corroborate the results of our thermal expansion measurements.

Collecting the anomalies found in dilatometric and magnetic quantities allows for the construction of the magnetoelastic phase diagram shown in Fig. 4 (see the Supplemental Material [21] for the magnetic measurements). In agreement with most phase diagrams reported in the literature [15,16], our dilatometric studies imply three distinct thermodynamic phases: Coming from the high-temperature paramagnetic (PM) regime the spin system undergoes a continuous phase transition into a canted antiferromagnetic (AFM) state at T_N. Upon increasing the magnetic field along the Co-Co bonds, $Na_2Co_2TeO_6$ exhibits a first-order phase transition showing strong signs of quantum criticality. Above B_C, the spins reorient (SR) out of their low-field configuration into a yet unknown magnetic structure while above $B_S(2\ \mathrm{K}) = 10$ T, the magnetic moments are almost fully polarized. As indicated by the shaded area in Fig. 4, the AFM/SR phase boundary exhibits pronounced hysteresis at low temperatures. At low temperatures, our data suggest that the system does not return into the AFM phase even when the magnetic field is decreased back to zero.

In conclusion, our measurements of the thermal expansion and magnetostriction consequently give insights into the important role of magnetoelastic coupling in the Kitaev candidate material $Na_2Co_2TeO_6$. A sign change of the Grüneisen parameter at the critical field B_C indicates the accumulation of entropy in the (B, T) plane above the critical field and thereby implies the existence of a metamagnetic QCEP. In addition, the proportional relationship between isothermal magnetization and magnetostriction for $B \leqslant B_C$ signals that the QCEP can be tuned by a magnetic field and pressure simultaneously. The presented results expand the scope of sample classes that exhibit metamagnetic quantum criticality to honeycomb antiferromagnets with possibly Kitaev-like interactions and, hence, contribute to the understanding of quantum criticality in antiferromagnetic insulating systems.

We acknowledge support by Deutsche Forschungsgemeinschaft (DFG) under Germany's Excellence Strategy EXC2181/1-390900948 (the Heidelberg STRUCTURES Excellence Cluster). J.A. acknowledges support by the IMPRS-QD Heidelberg. K.Y.C. was supported by the National Research Foundation (NRF) of Korea (Grants No. 2020R1A5A1016518 and No. RS-2023-00209121). R.S. acknowledges the financial support provided by the Ministry of Science and Technology in Taiwan under Project No. NSTC (113-2124-M-001-045-MY3 and 113-2124-M-001-003), Financial support from the Center of Atomic Initiative for New Materials (AI-Mat), National Taiwan University, (Project No. 113L900801) and Academia Sinica for the budget of AS-iMATE-113-12.

[1] A. Kitaev, Anyons in an exactly solved model and beyond, Ann. Phys. **321**, 2 (2006).

[2] G. Jackeli and G. Khaliullin, Mott insulators in the strong spin-orbit coupling limit: From Heisenberg to a quantum compass and Kitaev models, Phys. Rev. Lett. **102**, 017205 (2009).

[3] H. Takagi, T. Takayama, G. Jackeli, G. Khaliullin, and S. E. Nagler, Concept and realization of Kitaev quantum spin liquids, Nat. Rev. Phys. **1**, 264 (2019).

[4] S. Hwan Chun, J.-W. Kim, J. Kim, H. Zheng, C. C. Stoumpos, C. D. Malliakas, J. F. Mitchell, K. Mehlawat, Y. Singh, Y. Choi, T. Gog, A. Al-Zein, M. M. Sala, M. Krisch, J. Chaloupka, G. Jackeli, G. Khaliullin, and B. J. Kim, Direct evidence for dominant bond-directional interactions in a honeycomb lattice iridate Na_2IrO_3, Nat. Phys. **11**, 462 (2015).

[5] S.-H. Do, S.-Y. Park, J. Yoshitake, J. Nasu, Y. Motome, Y. S. Kwon, D. T. Adroja, D. J. Voneshen, K. Kim, T.-H. Jang, J.-H. Park, K.-Y. Choi, and S. Ji, Majorana fermions in the Kitaev quantum spin system α-$RuCl_3$, Nat. Phys. **13**, 1079 (2017).

[6] Y. Kasahara, T. Ohnishi, Y. Mizukami, O. Tanaka, S. Ma, K. Sugii, N. Kurita, H. Tanaka, J. Nasu, Y. Motome, T. Shibauchi,

and Y. Matsuda, Majorana quantization and half-integer thermal quantum Hall effect in a Kitaev spin liquid, Nature (London) **559**, 227 (2018).

[7] H. Liu and G. Khaliullin, Pseudospin exchange interactions in d^7 cobalt compounds: Possible realization of the Kitaev model, Phys. Rev. B **97**, 014407 (2018).

[8] R. Sano, Y. Kato, and Y. Motome, Kitaev-Heisenberg Hamiltonian for high-spin d^7 Mott insulators, Phys. Rev. B **97**, 014408 (2018).

[9] H. Liu, J. Chaloupka, and G. Khaliullin, Kitaev spin liquid in d^7 transition metal compounds, Phys. Rev. Lett. **125**, 047201 (2020).

[10] A. K. Bera, S. M. Yusuf, A. Kumar, and C. Ritter, Zigzag antiferromagnetic ground state with anisotropic correlation lengths in the quasi-two-dimensional honeycomb lattice compound $Na_2Co_2TeO_6$, Phys. Rev. B **95**, 094424 (2017).

[11] W. Chen, X. Li, Z. Hu, Z. Hu, L. Yue, R. Sutarto, F. He, K. Iida, K. Kamazawa, W. Yu, X. Lin, and Y. Li, Spin-orbit phase behavior of $Na_2Co_2TeO_6$ at low temperatures, Phys. Rev. B **103**, L180404 (2021).

[12] W. G. F. Krüger, W. Chen, X. Jin, Y. Li, and L. Janssen, Triple-q Order in $Na_2Co_2TeO_6$ from Proximity to Hidden-SU(2)-Symmetric Point, Phys. Rev. Lett. **131**, 146702 (2023).

[13] J. Chaloupka, G. Jackeli, and G. Khaliullin, Zigzag magnetic order in the iridium oxide Na_2IrO_3, Phys. Rev. Lett. **110**, 097204 (2013).

[14] G. Xiao, Z. Xia, W. Zhang, X. Yue, S. Huang, X. Zhang, F. Yang, Y. Song, M. Wei, H. Deng, and D. Jiang, Crystal growth and the magnetic properties of $Na_2Co_2TeO_6$ with quasi-two-dimensional honeycomb lattice, Cryst. Growth Des. **19**, 2658 (2019).

[15] W. Yao and Y. Li, Ferrimagnetism and anisotropic phase tunability by magnetic fields in $Na_2Co_2TeO_6$, Phys. Rev. B **101**, 085120 (2020).

[16] G. Lin, J. Jeong, C. Kim, Y. Wang, Q. Huang, T. Masuda, S. Asai, S. Itoh, G. Günther, M. Russina, Z. Lu, J. Sheng, L. Wang, J. Wang, G. Wang, Q. Ren, C. Xi, W. Tong, L. Ling, Z. Liu *et al.*, Field-induced quantum spin disordered state in spin-1/2 honeycomb magnet $Na_2Co_2TeO_6$, Nat. Commun. **12**, 5559 (2021).

[17] L. Xiang, R. Dhakal, M. Ozerov, Y. Jiang, B. S. Mou, A. Ozarowski, Q. Huang, H. Zhou, J. Fang, S. M. Winter, Z. Jiang, and D. Smirnov, Disorder-enriched magnetic excitations in a Heisenberg-Kitaev quantum magnet $Na_2Co_2TeO_6$, Phys. Rev. Lett. **131**, 076701 (2023).

[18] X. Hong, M. Gillig, W. Yao, L. Janssen, V. Kocsis, S. Gass, Y. Li, A. U. B. Wolter, B. Büchner, and C. Hess, Phonon thermal transport shaped by strong spin-phonon scattering in a Kitaev material $Na_2Co_2TeO_6$, npj Quantum Mater. **9**, 18 (2024).

[19] C. H. Lee, S. Lee, Y. S. Choi, Z. H. Jang, R. Kalaivanan, R. Sankar, and K.-Y. Choi, Multistage development of anisotropic magnetic correlations in the Co-based honeycomb lattice $Na_2Co_2TeO_6$, Phys. Rev. B **103**, 214447 (2021).

[20] E. Dufault, F. Bahrami, A. Streeter, X. Yao, E. Gonzalez, Q. Zhang, and F. Tafti, Introducing the monoclinic polymorph of the honeycomb magnet $Na_2Co_2TeO_6$, Phys. Rev. B **108**, 064405 (2023).

[21] See Supplemental Material at http://link.aps.org/supplemental/10.1103/PhysRevB.110.L140402 for additional information on the measurements and complementary dilatometric and magnetic data.

[22] R. Küchler, T. Bauer, M. Brando, and F. Steglich, A compact and miniaturized high resolution capacitance dilatometer for measuring thermal expansion and magnetostriction, Rev. Sci. Instrum. **83**, 095102 (2012).

[23] J. Werner, W. Hergett, M. Gertig, J. Park, C. Koo, and R. Klingeler, Anisotropy-governed competition of magnetic phases in the honeycomb quantum magnet $Na_3Ni_2SbO_6$ studied by dilatometry and high-frequency ESR, Phys. Rev. B **95**, 214414 (2017).

[24] S. Gass, P. M. Cônsoli, V. Kocsis, L. T. Corredor, P. Lampen-Kelley, D. G. Mandrus, S. E. Nagler, L. Janssen, M. Vojta, B. Büchner, and A. U. B. Wolter, Field-induced transitions in the Kitaev material α-$RuCl_3$ probed by thermal expansion and magnetostriction, Phys. Rev. B **101**, 245158 (2020).

[25] L. Viciu, Q. Huang, E. Morosan, H. Zandbergen, N. Greenbaum, T. McQueen, and R. Cava, Structure and basic magnetic properties of the honeycomb lattice compounds $Na_2Co_2TeO_6$ and $Na_3Co_2SbO_6$, J. Solid State Chem. **180**, 1060 (2007).

[26] E. Lefrançois, M. Songvilay, J. Robert, G. Nataf, E. Jordan, L. Chaix, C. V. Colin, P. Lejay, A. Hadj-Azzem, R. Ballou, and V. Simonet, Magnetic properties of the honeycomb oxide $Na_2Co_2TeO_6$, Phys. Rev. B **94**, 214416 (2016).

[27] M. Garst and A. Rosch, Sign change of the Grüneisen parameter and magnetocaloric effect near quantum critical points, Phys. Rev. B **72**, 205129 (2005).

[28] A. J. Millis, A. J. Schofield, G. G. Lonzarich, and S. A. Grigera, Metamagnetic quantum criticality in metals, Phys. Rev. Lett. **88**, 217204 (2002).

[29] P. Gegenwart, Grüneisen parameter studies on heavy fermion quantum criticality, Rep. Prog. Phys. **79**, 114502 (2016).

[30] C. Beneke and M. Vojta, Divergence of the Grüneisen ratio at symmetry-enhanced first-order quantum phase transitions, Phys. Rev. B **103**, 174420 (2021).

[31] S. Zhang, S. Lee, A. J. Woods, W. K. Peria, S. M. Thomas, R. Movshovich, E. Brosha, Q. Huang, H. Zhou, V. S. Zapf, and M. Lee, Electronic and magnetic phase diagrams of the Kitaev quantum spin liquid candidate $Na_2Co_2TeO_6$, Phys. Rev. B **108**, 064421 (2023).

[32] P. Gegenwart, F. Weickert, M. Garst, R. S. Perry, and Y. Maeno, Metamagnetic quantum criticality in $Sr_3Ru_2O_7$ studied by thermal expansion, Phys. Rev. Lett. **96**, 136402 (2006).

[33] S. A. Grigera, R. S. Perry, A. J. Schofield, M. Chiao, S. R. Julian, G. G. Lonzarich, S. I. Ikeda, Y. Maeno, A. J. Millis, and A. P. Mackenzie, Magnetic field-tuned quantum criticality in the metallic ruthenate $Sr_3Ru_2O_7$, Science **294**, 329 (2001).

[34] S. A. Grigera, P. Gegenwart, R. A. Borzi, F. Weickert, A. J. Schofield, R. S. Perry, T. Tayama, T. Sakakibara, Y. Maeno, A. G. Green, and A. P. Mackenzie, Disorder-sensitive phase formation linked to metamagnetic quantum criticality, Science **306**, 1154 (2004).

[35] C. Paulsen, A. Lacerda, J. Tholence, and J. Flouquet, Low temperature properties of heavy-fermion $CeRu_2Si_2$ studied by magnetization experiments, Phys. B: Condens. Matter **165–166**, 433 (1990).

[36] F. Weickert, M. Brando, F. Steglich, P. Gegenwart, and M. Garst, Universal signatures of the metamagnetic quantum critical endpoint: Application to $CeRu_2Si_2$, Phys. Rev. B **81**, 134438 (2010).

[37] J. Baier, P. Steffens, O. Schumann, M. Kriener, S. Stark, H. Hartmann, O. Friedt, A. Revcolevschi, P. G. Radaelli, S. Nakatsuji, Y. Maeno, J. A. Mydosh, T. Lorenz, and M. Braden, Magnetoelastic coupling across the metamagnetic transition in $Ca_{2-x}Sr_xRuO_4 (0.2 \leqslant x \leqslant 0.5)$, J. Low Temp. Phys. **147**, 405 (2007).

[38] V. Taufour, D. Aoki, G. Knebel, and J. Flouquet, Tricritical point and wing structure in the itinerant ferromagnet UGe_2, Phys. Rev. Lett. **105**, 217201 (2010).

[39] D. Aoki, T. Combier, V. Taufour, T. D. Matsuda, G. Knebel, H. Kotegawa, and J. Flouquet, Ferromagnetic quantum critical endpoint in UCoAl, J. Phys. Soc. Jpn. **80**, 094711 (2011).

[40] M. Uhlarz, C. Pfleiderer, and S. M. Hayden, Quantum phase transitions in the itinerant ferromagnet $ZrZn_2$, Phys. Rev. Lett. **93**, 256404 (2004).